Am. J. Hum. Genet. 63:1703–1711, 1998

Multiple Molecular Mechanisms Underlying Subdiagnostic Variants of Marfan Syndrome

Robert A. Montgomery,[1] Michael T. Geraghty,[2] Evelyn Bull,[2] Bruce D. Gelb,[5] Maureen Johnson,[6,*] Iain McIntosh,[3] Clair A. Francomano,[6] and Harry C. Dietz[2,4]

Departments of [1]Surgery, [2]Pediatrics, and [3]Medicine, and [4]Howard Hughes Medical Institute and Institute of Genetic Medicine, Johns Hopkins University School of Medicine, Baltimore; [5]Departments of Pediatrics and Human Genetics, Mount Sinai School of Medicine, New York; and [6]Medical Genetics Branch, National Human Genome Research Institute, National Institutes of Health, Bethesda

Summary

Mutations in the FBN1 gene, which encodes fibrillin-1, cause Marfan syndrome (MFS) and have been associated with a wide range of milder, overlap phenotypes. The factors that modulate phenotypic severity, both between and within families, remain to be determined. This study examines the relationship between the FBN1 genotype and phenotype in families with extremely mild phenotypes and in those that show striking clinical variation among apparently affected individuals. In one family, clinically similar but etiologically distinct disorders are segregating independently. In another, somatic mosaicism for a mutant FBN1 allele is associated with subdiagnostic manifestations, whereas germ-line transmission of the identical mutation causes severe and rapidly progressive disease. A third family cosegregates mild mitral valve prolapse syndrome with a mutation in FBN1 that can be functionally distinguished from those associated with the classic MFS phenotype. These data have immediate relevance for the diagnostic and prognostic counseling of patients and their family members.

Introduction

Marfan syndrome (MFS; MIM 154700) is a systemic disorder of connective tissue, with autosomal dominant inheritance and a prevalence of ~1/5,000–10,000 individuals (reviewed in Pyeritz 1993). The cardinal features of MFS involve the ocular, skeletal, and cardiovascular systems. The syndrome shows complete penetrance but is notable for variability in the timing of onset, tissue distribution, and severity of clinical manifestations, both between and within affected families. The ability to study the molecular determinants of phenotypic variation have become possible only since the identification of the fibrillin-1 gene (FBN1) as the site of primary mutations (Dietz et al. 1991; reviewed in Dietz and Pyeritz 1995). Fibrillin-1 monomers associate to form complex extracellular macroaggregates, termed "microfibrils," that are important for the integrity and homeostasis of both elastic and nonelastic tissues (Sakai et al. 1986; Pereira et al. 1997).

Mutations in FBN1 have been associated with a broad spectrum of phenotypes (reviewed in Dietz and Pyeritz 1995). The severe end of this clinical continuum is defined by a rapidly progressive form of MFS that presents at birth and that is associated with significant functional impairment and often death in early childhood. So-called classic MFS is a highly variable condition with pleiotropic manifestations in the eye (myopia and lens dislocation), skeleton (bone overgrowth and joint laxity), cardiovascular system (mitral valve prolapse and aortic dilatation and dissection), skin (striae distensae), and integument (hernia and dural ectasia). Conditions at the mild end include the MASS (mitral valve prolapse, borderline and nonprogressive aortic dilatation, and skin and skeletal manifestations) phenotype (MIM 157700), mitral valve prolapse syndrome (MIM 157700), isolated dolichostenomelia, predominant aortic aneurysm (MIM 132900), and ectopia lentis (MIM 129600) with relatively mild skeletal features. Because of the high population frequency and nonspecific nature of many of the clinical findings in MFS, clinical diagnostic criteria for this disorder have been established (De Paepe et al. 1996).

In this study, we examined the FBN1 genotype and cellular phenotype in families segregating MFS with marked intrafamilial clinical variability or with mild phenotypes that failed to meet diagnostic criteria for this disorder. Multiple molecular mechanisms, including so-

Received April 28, 1998; accepted for publication October 14, 1998; electronically published November 20, 1998.

Address for correspondence and reprints: Dr. Harry C. Dietz, Ross 1170, Johns Hopkins Hospital, 720 Rutland Avenue, Baltimore, Maryland 21205. E-mail: hdietz@welchlink.welch.jhu.edu

* Present affiliation: National Cancer Institute, National Institutes of Health, Bethesda.

0002-9297/98/6306-0017$02.00

matic mosaicism and allelic and locus heterogeneity, were identified as determinants of clinical expression.

Subjects and Methods

Subjects

This study was approved by an institutional review board, and informed consent was obtained. All participants were evaluated by a multidisciplinary team, including a medical geneticist, a cardiologist, and an ophthalmologist. Data obtained included family history, physical examination, and the results of echocardiography and slit-lamp examination. Control subjects for the population screening of mutation R1170H were unrelated and of Irish descent. Samples had been sent to a DNA diagnostic facility for the consideration of phenotypes other than MFS or for other heritable disorders of connective tissue. We remain unaware of the identity of these individuals.

Linkage Analysis

Linkage analysis was performed by use of microsatellite markers within the FBN1 gene. The primer sequences and assay conditions have been described elsewhere (Pereira et al. 1994). Haplotypes were generated by observing for combinations of marker alleles that segregated as a unit.

Mutation Identification and Population Screening

PCR amplification of individual exons of FBN1, heteroduplex analysis, and DNA sequencing were performed by use of primer sequences and conditions that have been described elsewhere (Nijbroek et al. 1995). Population screening for mutations C1265R, R1170H, and R529X was performed by use of restriction enzymes *Cac*8I, *Msc*I, and *Dde*I, respectively. All restriction enzymes were used in accordance with protocols supplied by the manufacturer (New England Biolabs).

Quantification of Mutant Transcript

RNA extraction, reverse-transcription PCR, and allele-specific oligonucleotide (ASO) hybridization analysis for mutation R529X were performed by use of standard procedures, without modification (Dietz et al. 1992). The primers used to amplify fibroblast or lymphoblast cDNA were FB5S (5′-TTACCGGTGTGAGTGCAAC-3′) and FB5AS (5′-AGGAGCCATCAGTGTTGAC-3′). The probes used for ASO analysis were R529-WT (5′-ACGCGGACAGAATGCCGAG-3′) and X529-MUT (5′-CTCAGCATTCTGTCCGCGT-3′). The final wash temperature for both probes was 62°C. Signal strength was quantified by use of the INSTANTIMAGER system (Packard Instrument). A correction factor was calculated in order to equalize the wild-type and mutant signals observed after sequential hybridization of the probes to PCR-amplified genomic DNA from an individual who had inherited R529X through germ-line transmission. This served to adjust for varying affinity of the two probes for their target sequences. This same correction factor was applied when determining the relative amount of wild-type and mutant signals in genomic DNA from an individual mosaic for R529X and in PCR-amplified cDNA.

As an alternative method for determination of the degree of mosaicism in the mother of the proband harboring R529X, genomic DNA derived from fibroblasts or from lymphoblasts was amplified with primers exon12S (5′-AGAATTATGAGGTATTGCTATG-3′) and exon12AS (5′-CAGTTAGCATATATGTCCCAC-3′). Cold and radioactive dCTP were included in the reaction mix, at final concentrations of 20 mM and 0.25 mM, respectively. The experiment was executed with 20, 25, and 30 cycles of amplification. Amplicons were digested with *Dde*I and were electrophoresed on an 8% polyacrylamide gel. The signal strength of each restriction fragment was measured by use of the INSTANT-IMAGER system.

Immunohistochemistry

Cell culture and immunohistochemical analysis were performed by use of procedures and reagents described elsewhere (Eldadah et al. 1995). Chamber slides were seeded with 2×10^5 cells from each culture and were grown for 72 h, prior to analysis. At this point all cultures had reached a comparable degree of cell density, as was confirmed by direct visualization and cell counting.

Results

Intrafamilial Genetic Heterogeneity

The proband (I-1) of the pedigree shown in figure 1*A*, who is now 32 years of age, was diagnosed with MFS in late adolescence because dolichostenomelia, arachnodactyly, pes planus, bilateral superior lens subluxation, and significant and progressive aortic root dilatation were found. Her eldest child (II-1) was 12 years of age and showed many suggestive features of a connective-tissue disorder, including a decreased upper-to-lower segment ratio (0.84), increased arm span–to-height ratio (1.05), arachnodactyly (middle-finger length >97%), a narrow and elongated face, pes planus, and an aortic annulus measurement that was 2.37 SDs above the mean, when standardized to age and body surface area. Aortic measurements at the sinuses of Valsalva, sinotubular junction, and ascending aorta were within normal limits. There was no pectus deformity, scoliosis, joint

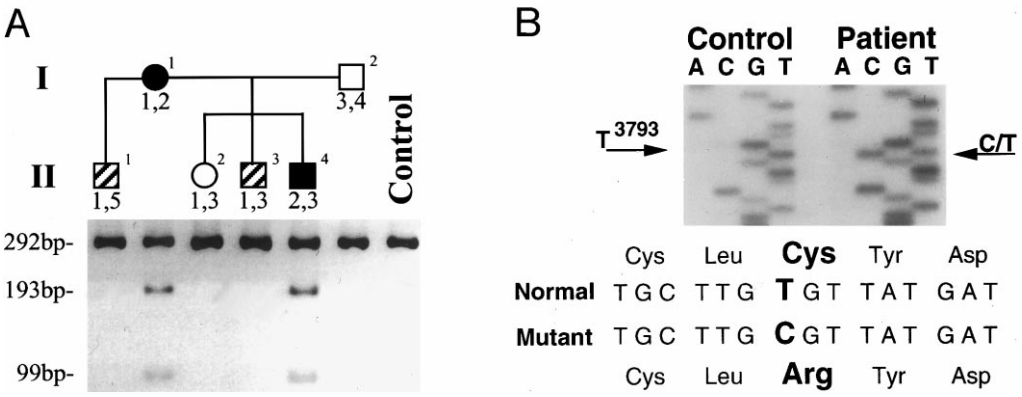

Figure 1 Analysis of mutation C1265R. *A,* Pedigree of a family displaying a heritable disorder of connective tissue. Blackened symbols indicate individuals with significant skeletal involvement and dilatation of the aortic root, with (I-1) or without (II-4) lens dislocation; hatched symbols indicate individuals with significant skeletal involvement and isolated dilatation of the aortic annulus (II-1) or of the ascending aorta, distal to the root (II-3); and unblackened symbols indicate no features of a connective-tissue disorder. Numbers designating FBN1 haplotypes are shown below each symbol. The results of restriction analysis for mutation C1265R are shown below the pedigree. The appearance of 193-bp and 99-bp restriction fragments manifests the presence of mutation C1265R. *B,* Sequence of PCR-amplified genomic DNA from individual I-1, showing a T→C transition at nucleotide 3793 in one allele. The exon sequence and the corresponding amino acid sequence of the normal and mutant alleles in the region of the mutation are shown (*bottom*), demonstrating a substitution of arginine ("Arg") for cysteine ("Cys") at codon 1265.

laxity, myopia, lens dislocation, or mitral valve prolapse. Three younger children were born to a different father (I-2). The eldest child (II-2) was 6 years of age and had an entirely normal physical exam, ophthalmology evaluation, and echocardiographic study. II-3 was 4 years of age and had a normal upper-to-lower segment ratio (1.17) but a mildly increased arm span–to-height ratio (1.04). He also had pes planus and pectus excavatum deformity but no arachnodactyly. He did not have myopia or lens dislocation. The echocardiogram showed a normal size for the aortic annulus and aortic root at the level of the sinuses of Valsalva. Dilatation of the aorta began at the sinotubular junction and extended through the ascending aortic arch (2.05 and 2.50 SDs, respectively, above the mean). There was no significant valvular regurgitation and no mitral valve prolapse. He had normal visual acuity, without lens dislocation. The youngest child (II-4) was 2 years of age. He had a normal upper-to-lower segment ratio of 1.06, an increased arm span–to-height ratio of 1.05, arachnodactyly, joint laxity, and malar hypoplasia. An echocardiogram revealed myxomatous mitral leaflets but no mitral valve prolapse or regurgitation. The aortic annulus, root, sinotubular junction, and ascending segment were significantly dilated (2.95, 5.78, 4.64, and 2.18 SDs, respectively, above the mean). There was no lens dislocation. Prior to molecular analysis, the referring physician had diagnosed the mother and her two youngest children (II-3 and II-4) with MFS. Despite the fact that the findings for the oldest child (II-1) were somewhat atypical and nonspecific, the diagnosis of MFS was strongly considered, because of the clinical presentation of other family members.

Haplotype segregation analysis using four intragenic microsatellite polymorphic markers revealed that the proband and her three apparently affected children did not all share a common FBN1 allele (fig. 1*A*). Heteroduplex analysis of a genomic amplicon from the proband, spanning exon 30 of the FBN1 gene, demonstrated an abnormally migrating fragment (data not shown). Direct sequencing of this amplicon revealed a T→C transition at nucleotide 3793 of the fibrillin-1 coding sequence, predicting the substitution of arginine (R) for cysteine (C) at codon 1265 (fig. 1*B*), within a calcium-binding epidermal growth factor–like (cbEGF-like) domain of fibrillin-1. Mutation C1265R creates a restriction site for enzyme *Cac*8I, cleaving the 292-bp amplicon into fragments of 193 bp and 99 bp. Restriction analysis revealed that the proband (I-1) and her son with classic distribution of aortic involvement (II-4) carry this mutation, whereas her two sons with significant skeletal involvement but atypical vascular manifestations (II-1 and II-3) and her unaffected daughter (II-2) do not (fig. 1*A*).

"Conservative" Mutation in FBN1

The proband (II-3) of the pedigree shown in figure 2*A*, who is now 46 years of age, was diagnosed with a nonspecific connective-tissue disorder because dolichos-

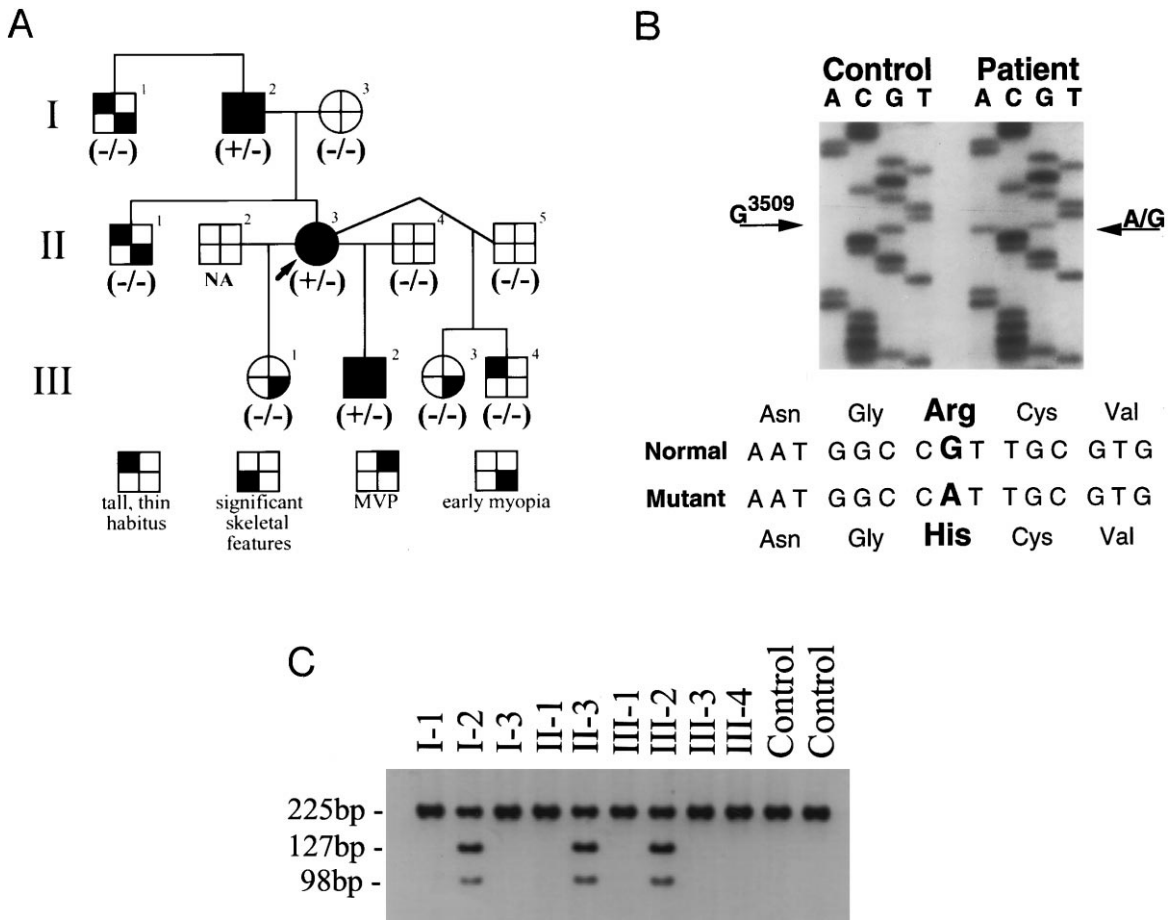

Figure 2 Analysis of mutation R1170H. *A,* Pedigree of a family displaying a heritable disorder of connective tissue. The key for the assignment of clinical features to each individual is shown below the pedigree. The proband (II-3) is indicated by an arrow. The FBN1 genotype is shown immediately below each symbol, with a plus sign (+) denoting the presence of R1170H on one allele. *B,* Sequence of PCR-amplified genomic DNA from individual II-3, showing a G→A transition at nucleotide 3509 in one allele. The exon sequence and the corresponding amino acid sequence of the normal and mutant alleles in the region of the mutation are shown (*bottom*), demonstrating a substitution of histidine ("His") for arginine ("Arg") at codon 1170. *C,* Results of restriction analysis for mutation R1170H. The appearance of 127-bp and 98-bp restriction fragments manifests the presence of mutation R1170H.

tenomelia, joint hypermobility, kyphoscoliosis, pes planus, positive wrist and thumb signs, striae distensae, early myopia, and myxomatous mitral leaflets with mitral valve prolapse were found. There was no lens dislocation, and all aortic measurements were within normal limits, when standardized to age and body surface area. As shown in figure 2*A*, multiple family members—including all four of the proband's children and her brother, father, and paternal uncle—had a tall, thin body habitus and/or preadolescent myopia. Two individuals, the proband's father (I-2) and eldest son (III-2), showed more-specific findings, including arachnodactyly, dolichostenomelia, pectus deformity, scoliosis, positive wrist and thumb signs, and mitral valve prolapse. Like the proband, neither of these individuals had lens dislocation or aortic dilatation. Although no individual in this family satisfied the diagnostic criteria for MFS (De Paepe et al. 1996), the proband and her father and eldest son likely share a mutant allele that caused an autosomal dominant disorder of connective tissue.

Heteroduplex analysis of a genomic amplicon from the proband, spanning exon 28 of the FBN1 gene, demonstrated an abnormally migrating fragment (data not shown). Direct sequencing of this amplicon revealed a G→A transition at nucleotide 3509 of the fibrillin-1 coding sequence, predicting the substitution of histidine (H) for arginine (R) at codon 1170 (fig. 2*B*), within a cbEGF-like domain of fibrillin-1. Mutation R1170H creates a restriction site for enzyme *Msc*I, cleaving the 225-bp amplicon into fragments of 127 bp and 98 bp. Restriction analysis revealed that all family members with significant skeletal involvement and mitral valve prolapse

carry this mutation, whereas individuals with only mild and nonspecific findings do not (fig. 2*C*). The proband's father was of Irish descent. We screened 100 samples, obtained from unrelated Irish individuals, that were sent to a DNA diagnostics facility for evaluation of a diagnosis other than MFS. Restriction analysis and sequencing revealed that only one patient, who was referred in order to rule out fragile X syndrome, was heterozygous for R1170H (data not shown). Although we were blinded to the identity of this individual, we know that the diagnosis of fragile X was excluded. No further information was available.

Somatic Mosaicism

The proband of the third family (fig. 3*B*) was diagnosed with MFS at 24 years of age, when an echocardiogram revealed dilatation of the aortic root, to 8 cm, and chronic ascending aortic arch dissection. Associated features included preadolescent myopia, dolichostenomelia, asymmetric pectus carinatum deformity, scoliosis, joint hypermobility, pes planus, and widespread striae distensae. There was no lens dislocation. The proband's mother, who is now 60 years of age, showed only joint hypermobility, pes planus, and striae distensae over the abdomen and trunk. There was no myopia or lens dislocation, and all aortic measurements were within normal limits, when standardized to age and body surface area. There was no other family history suggestive of a connective-tissue disorder.

Heteroduplex analysis of a genomic amplicon from the proband, spanning exon 12 of the FBN1 gene, demonstrated an abnormally migrating fragment (data not shown). Direct sequencing of this amplicon revealed a C→T transition at nucleotide 1585 of the fibrillin-1 coding sequence, predicting the substitution of a premature-termination codon (X) for arginine (R) at codon 529 (fig. 3*A*), within a cbEGF-like domain of fibrillin-1. Mutation R529X creates a restriction site for enzyme *Dde*I, cleaving the 223-bp amplicon into fragments of 170 bp and 53 bp. Remarkably, restriction analysis of PCR-amplified genomic DNA derived from lymphoblasts revealed that both the classically affected proband and his apparently unaffected mother harbor this nonsense mutation (fig. 3*B*). The decrease in intensity of the abnormal restriction fragment in the mother, relative to that seen in her son, suggests that she might be a somatic mosaic for mutation R529X. This hypothesis was tested by ASO analysis of PCR-amplified genomic DNA derived from lymphoblasts and cultured dermal fibroblasts (fig. 3*C*). The mutant signal was 27% and 34% of wild type in lymphoblasts and fibroblasts, respectively, which is consistent with ~43% of lymphoblasts and ~51% of fibroblasts having one R529X allele. Similar results were obtained by direct incorporation of radiolabel into genomic amplicons, after 20, 25, and 30 cycles of amplification; subsequent restriction digestion; and direct quantification of allele-specific signals (data not shown). Values were remarkably similar regardless of the number of cycles and suggested that 47.0% ± 3.5% and 60.7% ± 3.1% of lymphoblasts and fibroblasts, respectively, harbor the mutant allele. ASO analysis of reverse-transcription PCR–amplified cDNA from cultured fibroblasts showed that the mutant signal was 2% and 7% of wild type in the mother and the son, respectively (fig. 3*C*). This dramatic reduction in representation of the mutant allele can be attributed to the targeted degradation of transcripts harboring a premature-termination codon by the nonsense-mediated RNA-decay (NMRD) pathway (Dietz et al. 1993*a;* reviewed in Maquat 1995). Immunohistochemical analysis of cultured fibroblasts from the individual with somatic mosaicism revealed patchy deposition, in the extracellular matrix, of fibrils composed of fibrillin-1, when compared with that in control cultures (fig. 4). In contrast, cultured fibroblasts from this individual's son, who had inherited the nonsense mutation by germ-line transmission, showed nearly absent extracellular fibrillin-1 and no organized fibrils.

Discussion

Primary mutations in fibrillin-1 have been associated with a wide range of phenotypes that show considerable variation in the timing of onset, tissue distribution, and severity of clinical manifestations (reviewed in Dietz and Pyeritz 1995). Many of these conditions, such as mitral valve prolapse syndrome, MASS phenotype, or isolated skeletal disorders, show significant overlap with MFS and are quite common in the general population. In order to facilitate appropriate patient management and counseling, clinical criteria for the diagnosis of MFS were established (Beighton et al. 1988; De Paepe et al. 1996). Initial criteria (Beighton et al. 1988) proved to be too lenient, allowing the inappropriate diagnosis of individuals who had some manifestations of a connective-tissue disorder and a positive family history for MFS but who lacked serious and specific manifestations of MFS and ultimately were shown not to carry the fibrillin-1 mutation seen in more classically affected relatives (Pereira et al. 1994; Nijbroek et al. 1995). Revised diagnostic criteria (De Paepe et al. 1996) now require at least one of four manifestations with major diagnostic significance (lens dislocation, aortic dilatation or dissection, dural ectasia, or a specified combination of skeletal features) and involvement of at least one other system, for MFS to be diagnosed in an individual with an unequivocally affected first-degree relative.

Although vascular disease in MFS can involve any segment of the aorta, the root of the aorta is the most

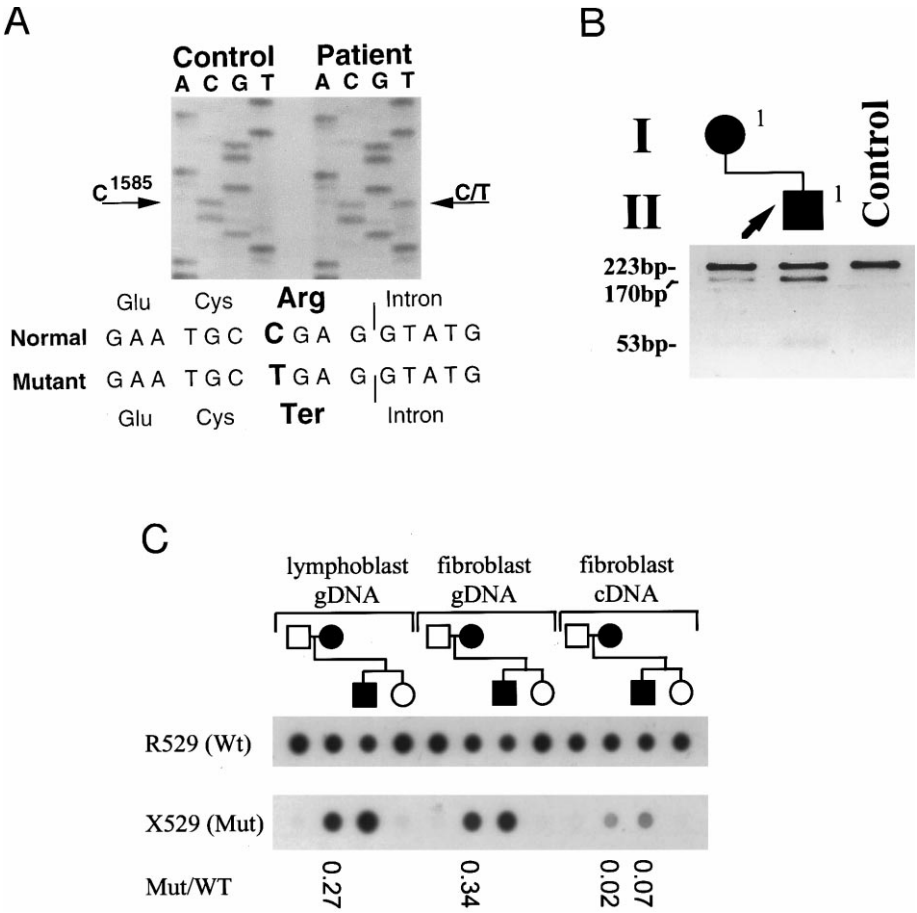

Figure 3 Analysis of mutation R529X. *A,* Sequence of PCR-amplified genomic DNA from individual II-1 (see panel *B*), showing a C→T transition at nucleotide 1585 in one allele. The gene sequence and the corresponding amino acid sequence of the normal and mutant alleles in the region of the mutation are shown (*bottom*), demonstrating a substitution of a termination codon ("Ter") for arginine ("Arg") at codon 529. *B,* Negative image of an ethidium bromide–stained gel, showing results of restriction analysis for mutation R529X. The appearance of 170-bp and 53-bp restriction fragments manifests the presence of the mutation. Note that the intensity of the abnormal restriction fragments is lower in the sample from I-1, compared with that in the sample from the proband (II-1), suggesting that I-1 is a somatic mosaic. *C,* ASO-hybridization analysis of PCR-amplified lymphoblast or fibroblast genomic DNA ("gDNA") or fibroblast cDNA, from the indicated members of the third family studied. The numbers at the bottom indicate the mutant-to–wild-type signal ratio after application of a correction factor used to equalize the signals observed in the gDNA samples from the proband.

typical site of dilatation and dissection. The new diagnostic criteria take this into consideration by allowing only dilatation that includes at least the sinuses of Valsalva to be of "major" diagnostic significance (De Paepe et al. 1996). This is relevant to the family shown in figure 1. The conclusion that neither child with an atypical pattern of aortic involvement carried the same genetic predisposition as relatives with dilatation at the sinuses of Valsalva was validated by mutation analysis. These individuals, who would have met the old diagnostic criteria for MFS (Beighton et al. 1988), clearly need an individualized approach to counseling and management.

Although there is ample evidence for a dominant-negative mechanism in MFS, the aspects of pathogenesis that relate to clinical variability are poorly understood. The majority of mutations occur within the 47 tandemly repeated EGF-like domains of fibrillin-1, of which 43 satisfy the consensus for calcium binding (Handford et al. 1991; Selander-Sunnerhagen et al. 1992; Corson et al. 1993; Pereira et al. 1993). Nearly all of these mutations substitute one of the six predictably spaced cysteine residues that interact via intradomain disulfide linkage, one of the highly conserved residues within the calcium-binding consensus sequence, or residues important for interdomain hydrophobic packing interactions (Dietz and Pyeritz 1995; Downing et al. 1996). Solving for the solution structure of a pair of cbEGF-like domains of fibrillin-1 documented that calcium binding is required, to maintain a rigid, rodlike structure for tandemly repeated motifs (Downing et al. 1996; Knott et

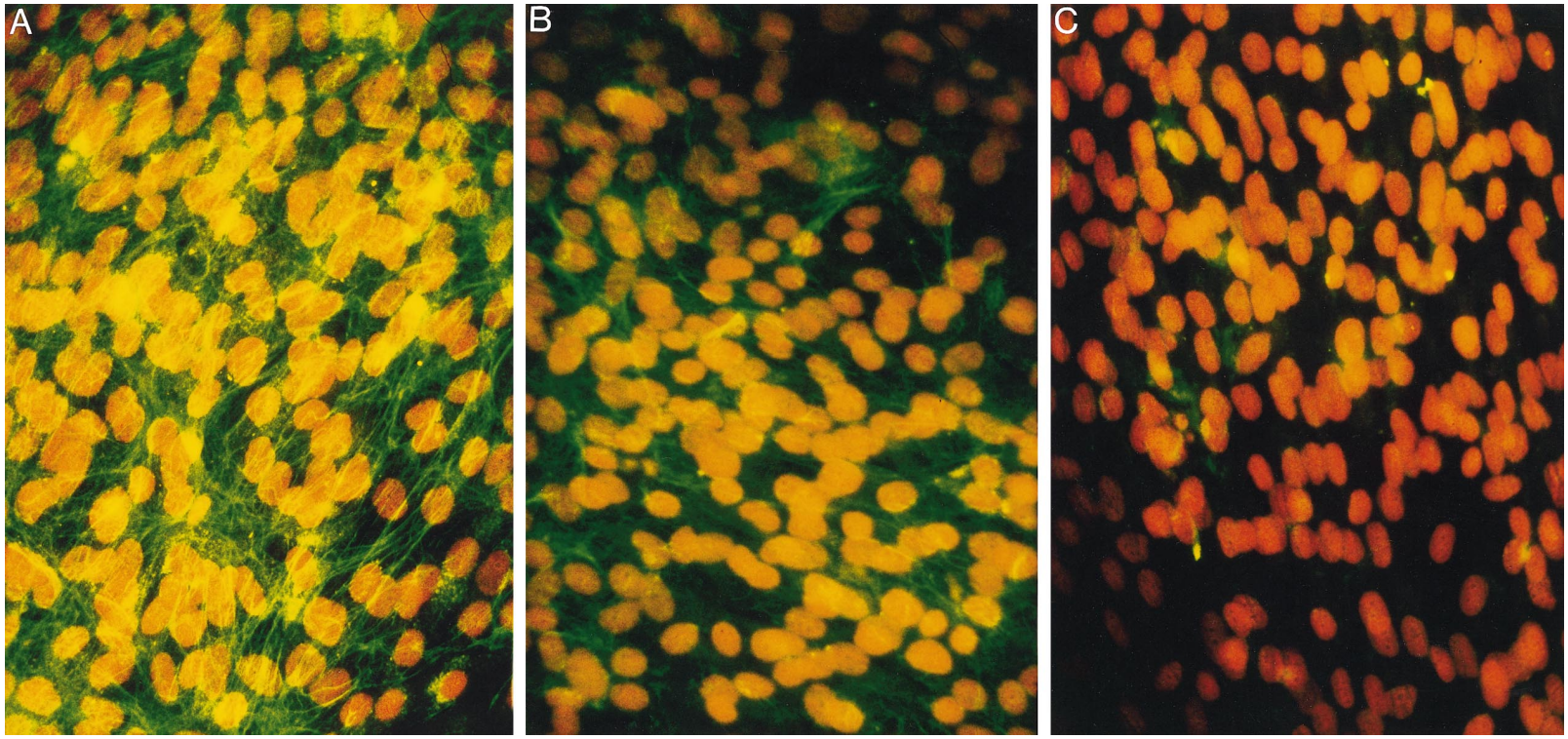

Figure 4 Immunohistochemical analysis using a monoclonal antibody directed against fibrillin-1 and cultured dermal fibroblasts from (*A*) a control individual and from (*B*) individual I-1 and (*C*) the proband (II-1) from the third family. Nuclei are stained orange, with propidium iodide. Extracellular fibrillin-1 appears green. Deposition is dense and diffuse in the control specimen, patchy in the sample from I-1, and nearly absent in the sample from II-1.

al. 1996). Moreover, perturbation of domain folding or calcium binding has been shown to result in conformational changes and enhanced proteolytic degradation of single domains, recombinant peptides or intact monomers, and ultrastructural changes in microfibrils (Kielty and Shuttleworth 1993, 1994; Wu et al. 1995; Reinhardt et al. 1997*a,* 1997*b*).

If only a handful of residues in EGF-like domains have functional significance and are mutated in MFS, then why are nearly all the intervening residues in human fibrillin-1 identical in mouse, pig, and cow (Tilstra et al. 1994; Yin et al. 1995; authors' unpublished data)? With one exception, the few mutations in these intervening regions of EGF-like domains of fibrillin-1 involve cysteine, proline, or glycine residues and therefore are predicted, or have been proved, to alter domain folding (Dietz and Pyeritz 1995; Wu et al. 1995; Downing et al. 1996). The remaining, and potentially most interesting, mutation (R1170H) falls in a variable loop region and was shown to cosegregate with an isolated skeletal phenotype in a small family (Hayward et al. 1994). It has been postulated that such a mutation allows the deposition of stable microfibrils with relatively preserved structure and function (Hayward et al. 1994; Downing et al. 1996). We now have shown that R1170H cosegregates with disease in a second family displaying a phenotype that predominantly involves the skeleton. These data suggest that residues within the variable loop regions of EGF-like domains in fibrillin-1 have functional significance and that events modulated by R1170, within the EGF-like domain encoded by FBN1 exon 28, influence skeletal growth.

In the third family, the individual who had inherited R529X through germ-line transmission displayed a classic and severe MFS phenotype, despite the marked decrease in mutant-transcript abundance induced by this nonsense mutation. Nonsense mutations in FBN1 and many other genes have been shown to induce mutant-transcript degradation, through NMRD (Dietz et al. 1993*a;* reviewed in Maquat 1995). Selected FBN1 nonsense alleles have been shown to be associated with mild phenotypes, whereas others have been shown to produce severe disease (Dietz et al. 1993*a,* 1993*b;* Aoyama et al. 1994). The genotype-specific efficiency of NMRD has been proposed to be the discriminating factor. It has been suggested that mutant-transcript levels $\gtrsim$10% of wild type may produce a protein sufficiently truncated to allow dominant-negative interference with the utilization of protein derived from the wild-type allele. Thus far, the 7% level of mutant transcript seen with R529X is the lowest to be associated with severe MFS. Immunohistochemical analysis of cultured dermal fibroblasts from the patient heterozygous for R529X showed a near absence of extracellular fibrillin-1. It is unclear whether this finding manifests dominant-negative activity of a trivial level of mutant protein or a protein concentration–dependent perturbation of matrix utilization of product from the wild-type allele.

It was very interesting to note the extremely mild phenotype observed in indivudual I-1 (fig. 3), who is a somatic mosaic for a fibrillin-1 mutation. The clinical samples only showed the mutation in ~50% of cells. Documented involvement of such embryologically diverse tissues as peripheral blood leukocytes, dermal fibroblasts, and the germ line suggests that all tissues are similarly affected. Immunohistochemical analysis of cultured dermal fibroblasts showed patchy deposition of extracellular fibrillin-1. These data have implications for gene therapy for this disorder, suggesting that $\leqslant$50% of cells would need to be corrected, to achieve a significant therapeutic benefit.

Acknowledgments

We thank Dr. Lynn Sakai for providing the monoclonal antibodies used in this study and for useful discussions. This work was supported by the Howard Hughes Medical Institute, the Smilow Family Foundation, the National Marfan Foundation, the Dana and Albert Broccoli Center for Aortic Diseases, and grant RO1-AR41135 from the National Institutes of Health (all supporting H.C.D.); the Division of Intramural Research and the National Human Genome Research Institute (support to M.J., I.M., and C.A.F.); and the American College of Surgeons Faculty Scholarship (to R.A.M.).

Electronic-Database Information

Accession numbers and URL for data in this article are as follows:

Online Mendelian Inheritance in Man (OMIM), http://www.ncbi.nlm.nih.gov/Omim (for MFS [MIM 154700], MASS phenotype and mitral valve prolapse syndrome [MIM 157700], predominant aortic aneurysm [MIM 132900], and ectopia lentis [MIM 129600])

References

Aoyama T, Francke U, Dietz HC, Furthmayr H (1994) Quantitative differences in biosynthesis and extracellular deposition of fibrillin cultured fibroblasts distinguish five groups of Marfan syndrome patients and suggest distinct pathogenetic mechanisms. J Clin Invest 94:130–137

Beighton P, De Paepe A, Danks D, Finidori G, Gedde-Dahl T, Goodman R, Hall JG, et al (1988) International nosology of heritable disorders of connective tissue. Am J Med Genet 29:581–594

Corson GM, Chalberg SC, Dietz HC, Charbonneau N, Sakai LY (1993) Fibrillin binds calcium and is encoded by cDNAs that reveal a multidomain structure and alternatively spliced exons at the 5′ end. Genomics 17:476–484

De Paepe A, Devereux RB, Dietz HC, Hennekam RCM, Pyeritz

RE (1996) Revised diagnostic criteria for the Marfan syndrome. Am J Med Genet 62:417–426

Dietz HC, Cutting GR, Pyeritz RE, Maslen CL, Sakai LY, Corson GM, Puffenberger EG, et al (1991) Marfan syndrome caused by a recurrent de novo missense mutation in the fibrillin gene. Nature 352:337–359

Dietz HC, McIntosh I, Sakai LY, Corson GM, Chalberg SC, Pyeritz RE, Francomano CA (1993*a*) Four novel FBN1 mutations: significance for mutant transcript level and EGF-like domain calcium binding in the pathogenesis of Marfan syndrome. Genomics 17:468–475

Dietz HC, Pyeritz RE (1995) Mutations in the human gene for fibrillin-1 (FBN1) in the Marfan syndrome and related disorders. Hum Mol Genet 4:1799–1809

Dietz HC, Pyeritz RE, Puffenberger EG, Kendzior RJ, Corson GM, Maslen CL, Sakai LY, et al (1992) Marfan phenotype variability in a family segregating a missense mutation in the epidermal growth factor–like motif of the fibrillin gene. J Clin Invest 89:1674–1680

Dietz HC, Valle D, Francomano CA, Kendzior RJ Jr, Pyeritz RE, Cutting GR (1993*b*) The skipping of constitutive exons in vivo induced by nonsense mutations. Science 259: 680–683

Downing AK, Knott V, Werner JM, Cardy CM, Campbell ID, Handford PA (1996) Solution structure of a pair of calcium-binding epidermal growth factor–like domains: implications for the Marfan syndrome and other genetic disorders. Cell 85:597–605

Eldadah ZA, Brenn T, Furthmayr H, Dietz HC (1995) Expression of a mutant fibrillin (FBN1) allele upon a normal human or murine genetic background recapitulates a Marfan cellular phenotype. J Clin Invest 95:874–880

Handford PA, Mayhew M, Baron M, Winship PR, Campbell ID, Brownlee GG (1991) Key residues involved in calcium binding motifs in EGF-like domains. Nature 351:164–167

Hayward C, Porteous ME, Brock DJ (1994) A novel mutation in the fibrillin gene (FBN1) in familial arachnodactyly. Mol Cell Probes 8:325–327

Kielty CM, Shuttleworth CA (1993) The role of calcium in the organization of fibrillin microfibrils. FEBS Lett 336: 323–326

——— (1994) Abnormal fibrillin assembly by dermal fibroblasts from two patients with Marfan syndrome. J Cell Biol 124:997–1004

Knott V, Downing AK, Cardy CM, Handford P (1996) Calcium binding properties of an epidermal growth factor–like domain pair from human fibrillin-1. J Mol Biol 255:22–27

Maquat LE (1995) When cells stop making sense: effects of nonsense codons on RNA metabolism in vertebrate cells. RNA 1:453–465

Nijbroek G, Sood S, McIntosh I, Francomano CA, Bull E, Pereira L, Ramirez F, et al (1995) Fifteen novel *FBN1* mutations causing Marfan syndrome detected by heteroduplex analysis of genomic amplicons. Am J Hum Genet 57:8–21

Pereira L, Andrikopoulos K, Tian J, Lee S-Y, Keene DR, Ono R, Reinhardt DP, et al (1997) Targeting of the gene encoding fibrillin-1 recapitulates the vascular aspect of Marfan syndrome. Nat Genet 17:218–222

Pereira L, D'Alessio M, Ramirez F, Lynch JR, Sykes B, Pangilinan T, Bonadio J (1993) Genomic organization of the sequence coding for fibrillin, the defective gene product in Marfan syndrome. Hum Mol Genet 2:961–968

Pereira L, Levra O, Ramirez F, Lynch JR, Sykes B, Pyeritz RE, Dietz HC (1994) A molecular approach to the stratification of cardiovascular risk in families with Marfan's syndrome. N Engl J Med 331:148–153

Pyeritz RE (1993) The Marfan syndrome. In: Royce PM, Steinmann B (eds) Connective tissue and its heritable disorders: molecular, genetic and medical aspects. Wiley-Liss, New York, pp 437–468

Reinhardt DP, Mechling DE, Boswell BA, Keene DR, Sakai LY, Bachinger HP (1997*a*) Calcium determines the shape of fibrillin. J Biol Chem 272:7368–7373

Reinhardt DP, Ono RN, Sakai LY (1997*b*) Calcium stabilizes fibrillin-1 against proteolytic degradation. J Biol Chem 272: 1231–1237

Sakai LY, Keene DR, Engvall E (1986) Fibrillin, a new 350-kD glycoprotein is a component of extracellular microfibrils. J Cell Biol 103:2499–2509

Selander-Sunnerhagen M, Ullner M, Persson E, Teleman O, Stenflo J, Drakenberg T (1992) How an epidermal growth factor (EGF)–like domain binds calcium. J Biol Chem 267: 19642–19649

Tilstra DJ, Li L, Potter KA, Womack J, Byers PH (1994) Sequence of the coding region of the bovine fibrillin cDNA and localization to bovine chromosome 10. Genomics 23: 480–485

Wu Y-S, Bevilacqua VLH, Berg JM (1995) Fibrillin domain folding and calcium binding: significance to Marfan syndrome. Chem Biol 2:91–97

Yin W, Smiley E, Germiller J, Sanguineti C, Lawton T, Pereira L, Ramirez F, et al (1995) Primary structure and developmental expression of Fbn-1, the mouse fibrillin gene. J Biol Chem 270:1798–1806